Challenging the Necessity of a Perfect Prior: Insights from a Replication and a Robustness Study of NeRP

Meha Goyal[1], Kriti Gupta[1], Danny Jiang[1], Elaine Liu[1], Sonika Potnis[1], Jenny Xu[1]

[1]University of Michigan
{mehag, kritig, jdanny, liuym, potnissa, jennyx}@umich.edu

Abstract

Computational medical imaging methods like computed tomography (CT) are essential for diagnoses and treatment planning, but obtaining high-quality images can be time-consuming due to the need for numerous projections to reconstruct the desired image with sufficient detail. Meanwhile, frequent or prolonged scanning exposes patients to potentially harmful radiation. Implicit Neural Representation Learning with Prior Embedding for Sparsely Sampled Image Reconstruction (NeRP) offers a solution by using a high-quality prior image to reconstruct sparsely sampled CT images, accelerating the acquisition. However, the impact of prior image quality on reconstruction performance has not been thoroughly explored.

Our study replicates NeRP's 2D CT reconstruction and extends it by evaluating the model's robustness to lowered prior image qualities. We test how prior image quality affects reconstruction performances by introducing Gaussian noise, sparse sampling, and spatial misalignment to prior images. Our results show that NeRP is robust to most types of noise, producing high-quality reconstructions even with noisy prior images. However, spatial misalignment and device bed inconsistencies degraded performance, highlighting the importance of accurate alignment and consistent imaging conditions. By demonstrating the feasibility of NeRP with lower-quality priors, this work demonstrates NeRP's potential to reduce radiation exposure from CT scanning and minimize acquisition time while identifying key areas for future research. These findings have significant implications for clinical applications, especially when high-quality priors are not available.

Introduction

Obtaining high-quality diagnostic medical images is a crucial but tough task in medical settings. Computed Tomography (CT) is frequently used in medical scenarios for disease diagnosis and radiation therapy treatment planning, so it is important to obtain high-quality CTs. Obtaining them requires the acquisition of projection data from numerous angles (dense sampling), making the scanning process very time-consuming. In other words, CT scans require multiple X-rays to construct detailed 3D images of the body. Patients often need to be repeatedly scanned at each step of treatment; this process can be slow and prolonged scanning exposes patients to harmful amounts of radiation from the X-rays. It can also be difficult to obtain good-quality scans due to noise from factors like patient movement. Although scan quality improves with higher doses of radiation, it must be balanced with health risks.

To minimize radiation exposure and acquisition time, reconstruction with sparsely sampled data (fewer projections) to produce high-quality scans is a very desirable but difficult task. Image reconstruction is modeled as an inverse problem by solving for an image using sensor measurements. However, to obtain artifact-free images, the measurement space must be densely sampled, which is fundamentally opposed to the setup of sparsely sampled image reconstruction that we are solving. To address this challenge, previous approaches incorporate domain knowledge, such as the structural biology of the human body, as prior information to enhance model performance.

A significant example of this domain approach is the NeRP model, proposed by (Shen, Pauly, and Xing 2022), which successfully reconstructs sparsely sampled images with a high-quality prior image, which is usually obtained at an early stage of treatment. Comparison across reconstruction methods was presented for 3-D CT reconstruction tasks, which showed NeRP outperformed other state-of-the-art algorithms and highlighted its contribution to the fields. Ablation studies were also conducted by assessing reconstruction performance with or without a prior, recognizing the importance of the pre-training stage. While these results showed that involving a prior is important, it is unclear if their model still functions as expected when only lower-quality priors are available due to real-world limitations. Therefore, we pose the following research question: **How does a reduction in the quality of prior images impact a model's ability to implicitly learn a neural representation to perform image reconstruction?**

We started our work by replicating the NeRP method, specifically for the 2-D CT reconstruction task. Using publicly available code on GitHub, we performed reconstructions on both the provided sample data and a public dataset containing lung CT scans. For the extension task, we augmented the prior images in various ways to simulate reduced quality and followed a similar reconstruction workflow for evaluation. While our initial hypothesis was that noisy priors would lead to significantly worse reconstructions, the experiments showed that performance degradation was minimal, confirming the robustness of the NeRP method. Addition-

ally, certain types of noise had a greater impact on performance than others, offering meaningful clinical insights.

Related Work

Deep learning (DL) methods have achieved impressive progress in image reconstruction thanks to their ability to learn from large-scale data. Zhu et al. (2018) introduced a CNN model that learns to map between the sensor and image domain to accelerate the reconstruction of MRIs (Zhu et al. 2018). DL methods conventionally use convolutional neural networks (CNNs) to map raw measurement signals to the reconstructed image domain. Large training datasets are required but are hard to obtain due to medical data privacy and cost. Other limitations of current deep-learning methods include brittle reconstructions that are sensitive to unseen subjects and poor generalization to other anatomical sites and image modalities (Antun et al. 2020).

To reduce the reliance on data, Gong et al. proposed the Deep Image Prior (DIP) framework for PET reconstruction that requires no pre-training datasets (Gong et al. 2019). Their method leverages a patient-specific prior image to update a neural network during iterative reconstruction. Integrating anatomical priors, they achieved improved performance over kernel-based methods in improving signal-to-noise ratios and image clarity. Their work demonstrates how unsupervised, prior-based deep learning can be used for personalized image reconstruction.

Generative adversarial models (GAN) have been used to improve the reliance of conventional methods on large datasets by incorporating prior domain knowledge. (Cafaro et al. 2023) also recognized the importance of prior and trained an unsupervised style-GAN to learn general CT representations before performing sparse reconstructions. Although GAN models improve image quality, their output can be unreliable due to their generated structures and details and synthetic nature.

NeRP addresses the weaknesses in these current methods with three key contributions: its high-quality reconstruction with prior embeddings, reduced reliance on large training datasets, and adaptability across modalities. NeRP achieves superior reconstruction results as embedding prior information into the neural network parameters significantly enhances reconstruction. Reformulating the reconstruction task as a continuous function optimization minimizes the need for large datasets, making the method more adaptable and efficient in real clinical applications. By reducing this data reliance, NeRP can also better generalize across different imaging modalities and anatomical sites.

While these prior studies emphasize leveraging domain knowledge or improving reconstruction models, our extension focuses on evaluating the impact of prior image quality on reconstruction accuracy. By introducing noise to prior images and analyzing the results, we aim to provide an in-depth understanding of the robustness of NeRP's prior-based reconstruction technique, contributing a novel perspective to the existing body of work.

A study by Zhang et al. explored prior image-based reconstruction techniques with a focus on scenarios where there is a mismatched attenuation between the prior and current images in a low-dose CT scan (Zhang et al. 2022). Their work proposed two schemes to handle the mismatch and tested their work similarly by simulating low-dose projection data and comparing the results with the ground truth. Our extension similarly explores the effect of an imperfect prior by adding noise to scans rather than using mismatched scans.

Background

CT Imaging and Radon Transform

For CT scans, X-rays are emitted to pass through the patient's body from different angles, and the signals are attenuated depending on the tissues they pass through. The received signals can be understood as captured projections from different angles and this forward process can be modeled by Radon Transform. A densely sampled acquisition typically provides enough measurements to reconstruct a high-resolution image of the field of interest. To minimize scanning time and limit radiation exposure, fewer measurements are desired. However, this sparse sampling results in reduced information in data, which can lead to artifacts or reduced image quality when reconstructing CT images. Addressing this challenge is critical, especially in clinical applications requiring accurate diagnostic imaging.

Traditional algorithms of converting sensor data into a CT image include filtered back projection (FBP) or iterative reconstruction approaches. These algorithms transform the raw sensor data—essentially line integrals of X-ray attenuation along specific paths—into a two- or three-dimensional representation of the scanned anatomy. However, with sparse data, traditional techniques like these often fail to produce high-quality images, necessitating more advanced methods like those leveraging deep learning.

Neural Representation Learning and Prior Embedding

In the context of medical image reconstruction, a prior refers to any auxiliary information that can assist in improving the reconstruction process. For our study, this prior takes the form of a previous CT image of the same patient. This prior provides additional structural and anatomical information that can help compensate for the lack of sensor data in the current scan. By embedding this prior into the reconstruction process, we can guide the reconstruction toward more accurate and clinically meaningful results.

Implicit neural representation (INR) learning is a technique where a neural network learns a continuous function that maps spatial coordinates to corresponding pixel or voxel intensities. Unlike traditional imaging representations that use explicit grids of pixel values, INR captures the image as a mathematical function, allowing for efficient and continuous reconstructions. In this project, INR is coupled with prior embedding, where the prior image is used as an additional input to guide the learning process. Leveraging both the spatial continuity modeled by INR and the anatomical information provided by the prior, our approach enhances the reconstruction quality of CT images obtained from sparsely sampled data.

Dataset

Our study utilizes publicly available chest CT image data from *The Cancer Imaging Archive (TCIA)*, specifically the *CT Images in COVID-19* dataset (An et al. 2020). This dataset contains retrospective, unenhanced chest CT scans from patients with confirmed COVID-19 infections, verified through Reverse Transcription Polymerase Chain Reaction (RT-PCR) testing. We selected 3 patients' data from the *sequential CT subset*, which includes both initial point-of-care scans and follow-up CTs.

For our project, we focused on one slice of one patient's CT scan, where high-quality depiction of lung structures exists. The 4D CT scans from the patient include temporal sequences of lung images, capturing motion dynamics. This allowed for a comprehensive evaluation of reconstruction algorithms, with the selected patient and slice providing optimal clarity and diagnostic relevance for our study.

Performance Metrics

To evaluate the performance of the reconstruction techniques, we use two standard metrics:

- **PSNR (Peak Signal-to-Noise Ratio):** PSNR quantifies the ratio of the maximum possible power of a signal to the power of corrupting noise. Higher PSNR values indicate better reconstruction quality, with less deviation from the ground truth image.
- **SSIM (Structural Similarity Index Measure):** SSIM evaluates the perceived quality of an image by comparing structural information between the reconstructed image and the ground truth. This metric accounts for luminance, contrast, and structural similarity, providing a holistic assessment of image quality.

Methodology, Results, and Discussion

The following section starts with a mathematical formulation of the reconstruction problem, following methodology details, design choices, and results and analysis.

Problem Formulation

The process of reconstructing a computational image can be formulated as an inverse problem by $y = Ax + e$. Here, x is the ground truth CT volume (a 2D slice in our case), and y is the sampled sensor signal. The matrix A is the forward process that produces the attenuated X-ray signals to be received (Radon transform in our case). The final term e is the acquisition noise - this could be any noise in real settings, like electronic noise produced by the scanning device. The reconstruction is to predict x^*, the recovered image, by:

$$x^* = \text{argmin}_{x'} E(Ax', y) + \rho(x) \tag{1}$$

In Eq. 1, Ax' represents the signal generated by an image x' through the forward process, and $E(Ax', y)$ measures the errors (L2 loss in our case) between it and the real sampled signal. In other words, x^* is retrieved by finding the image that is most likely to produce the collected signals. $\rho(x)$ is the regularizer term, which is used to characterize physical knowledge specific to different inverse problems.

Methodology & Model

To achieve the reconstruction task, we followed the NeRP model by (Shen, Pauly, and Xing 2022). In NeRP, a prior image is utilized to initialize the weights of a multi-layer perceptron during pre-training. Then, the network is trained with the sparsely sampled measurements to learn a mapping from coordinates to intensity values. Finally, the reconstructed image is retrieved by inferring the trained network across all spatial coordinates in the image field. Due to computing power limitations, we decided to focus on replicating a sub-task in the original paper - reconstruction of 2D CTs.

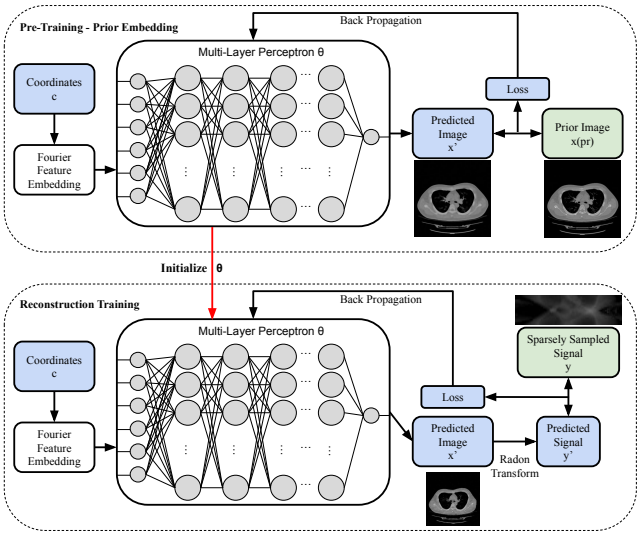

Figure 1: Methodology Graph Showing a Two-Stage Training Strategy Based on Multi-Layer Perceptron for Implicit Neural Representation Learning

Multi-Layer Perceptron As mentioned in the previous section, the model is essentially an implicit neural representation network implemented using the multi-layer perceptron (MLP), denoted M_θ with parameters θ. Given that Fourier features are shown to be helpful for high-frequency feature learning in (Tancik et al. 2020), the normalized coordinates c go through a Fourier feature mapping γ before being mapped to the intensity values. The mathematical formulation is as follows, with B being the coefficients for Fourier feature transformation:

$$\gamma(c) = [\cos(2\pi Bc), \sin(2\pi Bc)]^{\mathrm{T}}, c \in [0, 1)^n \tag{2}$$

$$M_\theta : \gamma(c) \mapsto v, v \in \mathrm{R} \tag{3}$$

The coordinates are simply grid values that are always available, so every trained MLP M_θ corresponds to exactly one CT image x, i.e. $x = M_\theta(\gamma(c))$. For simplicity, we will, from here, denote $x = M_\theta$. Combining the MLP formulation and the inverse problem formulation, we can turn the problem of finding an image into finding the optimal parameters to produce the image.

Prior Embedding The regularizer in the inverse formulation is implicitly included through an informed initialization

of the model in Eq. 4- fitting the continuous function represented by the MLP to a prior image x^{pr} (a previous CT scan) before actual reconstruction. In other words, pertaining finds ϕ^* to define an MLP that maps coordinates to intensity values in x^{pr}. These learned weights, M_{ϕ^*}, are then used to initialize the reconstruction network's parameters, implicitly embedding the prior image.

$$\phi^* = \text{argmin}_\phi E(M_\phi, x^{\text{pr}}) \tag{4}$$

This implicit regularization ensures all coordinates are mapped through the same underlying continuous function, which helps with the spatial continuity in the output domain. The formulation as a continuous function also regularizes the entire optimization process through neural representation learning.

Network Training & Reconstruction With the initialization parameters M_{ϕ^*} from pre-training, the final objective for network training can be formulated as Eq. 5, and the reconstruction result can be retrieved by Eq. 6.

$$\theta^* = \text{argmin}_{\theta'} E(AM_{\theta'}, y; M_{\phi^*}) \tag{5}$$

$$x^* = M_{\theta^*}(\gamma(c)) \tag{6}$$

To use the original paper's results as a benchmark for our replication results, we follow its hyper-parameter choices to perform our experiments. The same eight-layer MLP network with a width of 256 neural nodes is used for 2D CT reconstruction. The Fourier feature embedding size remains 256 with a hyper-parameter set as 4 for CT reconstruction. For prior embedding learning (optimizing Equation 4), the Adam optimizer with a learning rate of 0.0001 is used, and the network is trained for 1000 iterations. Then for the reconstruction network training, Equation 5 is optimized by training the MLP for 1000 iterations using the Adam optimizer with a learning rate of 0.00001. The networks are coded using PyTorch following the implementation provided by (Shen, Pauly, and Xing 2022).

Experiments & Results

For replication, three patients' lung CT scans were used. Each patient has two different CT scans obtained on different dates - the first scan was used as the prior image x^{pr} and the second as the reconstruction target x. The subsequent CT scan was sparsely sampled with the forward process (20 projections for the Radon transform) to obtain the sparsely sampled signal y shown in Figure 1.

To ensure data quality and successful replication, we preprocessed the data by clipping the HU values (CT intensity) to a range of -1024 to 2000, followed by min-max normalization to scale the values to a range of 0 to 1. Through experiments, we realized that the different shapes of the CT beds captured in our scans were major sources of noise and resulted in poor reconstruction quality. Noticing that the original paper had scans obtained with the same bed, we manually masked the beds in our scans to keep it consistent; the details will be further discussed in the next section. The images were then resized to 256 $\times$ 256 following the original implementation before entering the model. Finally, the reconstruction results were evaluated with PSNR and SSIM.

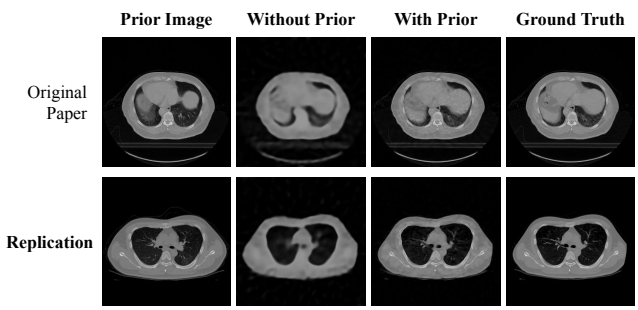

Figure 2: Results of 2-D CT image reconstruction in the original paper and replication with COVID lung CT data using 20 projections.

Following the original paper by (Shen, Pauly, and Xing 2022), we performed experiments on three patients separately and reconstructed the CT of each patient both with and without a prior. In the latter case, the model training started directly from the second stage with a random initialization of the MLP's parameters. The averaged metric values are reported in Table 1, along with those of the original paper. Note that we obtained the 2D metrics for NeRP in this table were obtained by running NeRP on the sample Patient 0 data provided by (Shen, Pauly, and Xing 2022).

	With Prior PSNR/SSIM	**Without Prior** PSNR/SSIM
Replication	30.42/0.734	28.61/0.623
NeRP 2D	34.87/0.886	27.08/0.660

Table 1: Results of 2D CT Image Reconstruction Using 20 Projections. Replication results are on the COVID Lung Dataset, and NeRP results are from (Shen, Pauly, and Xing 2022); Evaluation metrics reported include PSNR in dB and SSIM values.

Some image samples of the reconstruction results are shown in Figure 2. These visualizations illustrate the overall success of our replication. Our replication results, presented in the second row, exhibit a trend similar to that in the original paper—the reconstruction without prior results in a blurry outline, while the reconstruction with prior produces a high-quality image that retains most of the coarse details of the ground truth. Notably, our reconstruction with a prior reflects the detailed vessels in the target reconstruction image (ground truth) that differ from those in the prior. Additionally, the quantitative results in Table 1 show that pre-training with prior led to improvements in both reconstruction PSNR and SSIM, as anticipated. However, our reconstruction metrics with a prior were slightly inferior to the original implementation, which could have resulted from our lower-quality dataset. The dataset that was used by (Shen, Pauly, and Xing 2022) was collected specifically for this experiment, whereas the one used in our experiments is public.

To this point, we can confidently conclude that we successfully replicated the original NeRP model for the task of 2D CT reconstruction, proving its reproducibility.

Extensions

To extend NeRP, we test the robustness of the proposed model, focusing on how the quality of a prior image affects reconstruction quality. In this section, we state our extension's significance, provide implementation details, and analyze the results.

In practice, due to faulty equipment or other disturbances, available CT scans that could serve as potential priors are not always of high quality. For NeRP to effectively minimize CT acquisition time, it should ideally perform well even with lower-quality priors. However, to our knowledge, no published papers have specifically focused on the quality of the prior image. In the NeRP paper, ablation experiments were conducted only to compare the performance of models initialized with or without a prior. While these experiments highlighted the importance of the prior, they did not provide insight into whether the quality of the prior is a critical factor or if a low-quality prior could still yield satisfactory reconstructions.

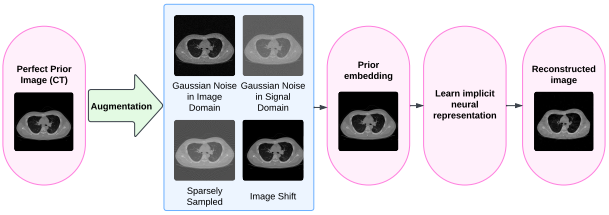

Figure 3: NeRP pipeline with our prior that was augmented by adding Gaussian noise in the image domain.

To test the impact of prior image quality, we performed robustness tests on one patient by separately introducing various types of noise to the prior and training the MLP on these priors. These "noises" included Gaussian noise in the image domain, Gaussian noise in the signal domain, sparsely sampled prior images, and shifted prior images. (Fig. 3). Since we tested NeRP's 2D image reconstruction capabilities on a COVID dataset, we chose one slice that was a good representation of the patients' lung anatomies as the input. Some results will be analyzed below, and a full table can be found in the Appendix.

It is worth noting that the shifting method differs from the other noise methods as it introduces spatial misalignment rather than additive noise. Consequently, the noise in the shifted prior is not well-represented by its PSNR, so its results should not be directly compared to the priors with added noise, even if they have the same PSNR. We will discuss the results of this method separately. Additionally, as highlighted in the previous section, we will briefly examine our discovery that device beds present in scans can also serve as potential noise sources.

Gaussian Noises and Sparse Sampling

First, we discuss the reconstruction results with priors altered by Gaussian noise in the image or the signal domain and the ones that were sparsely sampled.

Prior Type	PSNR(dB)	SSIM
Perfect Prior	30.89	0.821
Gaussian Noise (Image Domain)	30.80	0.819
Gaussian Noise (Signal Domain)	31.13	0.819
Sparse Sampling	31.32	0.848

Table 2: Results of 2D CT reconstruction with priors altered with different noises; Noisy priors have a PSNR $\approx$ 40dB.

To ensure a fair comparison across different types of noise in the prior, we evaluate results generated using augmented priors with a PSNR of 40dB, as presented in Table 2. According to the NeRP paper and other state-of-the-art models, a reconstruction PSNR of around 35dB is considered to be of desirable quality. Therefore, we believe this choice of noise level in the prior is reasonable. At this noise level, the priors resemble those shown in Figure 4B—blurry but are not entirely distorted. This aligns with the assumption that low-quality prior CT scans would retain sufficient detail for clinical diagnosis while not being rendered completely unusable.

While we anticipated that priors with lower PSNR values (more noise) would lead to poorer reconstruction quality, the reconstruction results, regardless of the noise added, were remarkably similar to those achieved with a perfect prior. As shown in Table 2, some noisy priors even produced slightly better reconstructions. Although this improvement was minimal and could be attributed to randomness in training, it is also possible that the added noise introduced randomness that helped mitigate over-fitting during pre-training. The limited differences in metrics were also visually negligible, as all reconstructions appeared similar to Figure 4C.

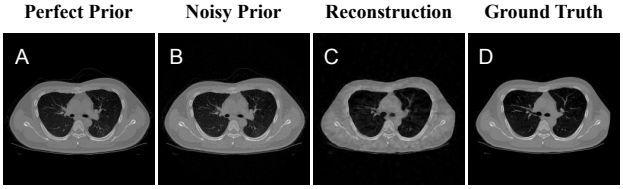

Figure 4: Sample reconstruction result with a prior augmented with noise in the signal domain, PSNR $\approx$ 26.72dB

Prior PSNR(dB)	Recon PSNR(dB)	Recon SSIM
Perfect Prior	30.89	0.821
26.72	30.14	0.740
35.26	30.99	0.794
40.13	31.12	0.819

Table 3: Results of 2D CT image reconstruction with priors altered with Gaussian noise in the signal domain.

Priors modified with the same type of noise but at different PSNR levels were also tested in reconstruction experiments, with selected results presented in Table 3 and Figure 4. Even with a prior PSNR as low as 26.72dB, the reconstruction quality was only marginally affected, further demonstrating the model's robustness.

Shifting

Next, we discuss the results of shifting the priors to introduce spatial misalignment between the prior and the measured data. This simulates the scenario where patient movement or equipment errors lead to poor registration of CT scans.

X-Shift(pixel)	PSNR(dB)	SSIM
0	30.89	0.821
5	30.67	0.826
10	29.41	0.735
20	28.74	0.668

Table 4: Results of 2D CT reconstruction with shifted priors.

To further evaluate the model's robustness under this setting, we applied horizontal shifts to the prior images by a set number of pixels. The MLP was then trained using these shifted priors, and the reconstructed images were compared with the ground truth. As shown in Table 4, as the shifting distance increased, both PSNR and SSIM decreased, indicating the model's sensitivity to spatial misalignment. This highlights the importance of accurate spatial alignment for achieving optimal NeRP reconstruction performance. Such sensitivity presents a notable challenge in medical image reconstruction, as real-world clinical settings often face unavoidable misalignment due to patient movement, breathing, or equipment variations.

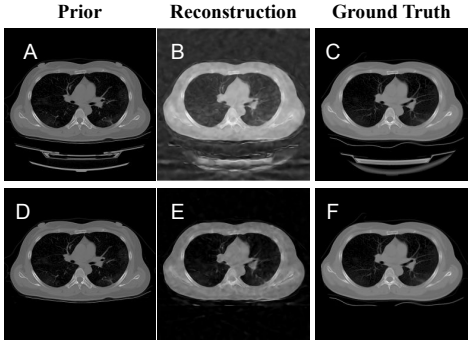

Figure 5: Comparison of 2D CT reconstruction with the device bed in the first row and without the device bed in the second row.

Device Bed as Noise

In initial replication trials, we encountered very poor results for one patient, as shown in the first row of Figure 5. The evaluation metrics were significantly lower than the NeRP results, with detailed values provided in the Appendix. Through analysis, we identified the differing shape of the device bed as a likely source of noise—a factor absent in the NeRP paper, where the same device bed was used for both images. To address this, we manually removed the device bed from both the prior and training images. Comparing images B and E in Figure 5, it is evident that the reconstruction of the anatomies improved after removing the device bed as it was free from distortions caused by varying bed shapes. This improvement is likely due to the implicit assumption of continuity in the underlying mapping, which is disrupted by abrupt changes in the device bed shape. Therefore, for real-world applications of NeRP, it is essential to ensure that the device bed either remains consistent in shape or is removed for reconstruction.

Conclusions

In this study, we successfully replicated the NeRP method for 2D CT image reconstruction to confirm the reproducibility of the original results. We also extended NeRP to test robustness against varying prior image quality, highlighting new insights and limitations regarding the impact of prior quality on reconstruction performance.

Through robustness tests, we found that priors altered with Gaussian noise or sparse sampling produced reconstructions comparable to those using perfect priors, expanding the possible application of the NeRP model. This indicates that the model's reliance on prior quality is less stringent than initially expected. Conversely, spatial misalignment introduced by shifting priors significantly degraded reconstruction quality, as evidenced by declining PSNR and SSIM metrics with increasing shift distances. Furthermore, we identified that variations in device bed shapes across scans can act as a major source of noise, distorting reconstructions. This finding highlights the need for consistent patient positioning and device bed configurations in NeRP implementations to ensure valid results.

However, these experiments have limitations, as the signal domain inputs used during reconstruction were generated through the forward process (Radon Transform), which may introduce additional errors. If time and resources permit, further testing with self-collected raw signals would be preferable to eliminate this potential source of error. Similarly, some prior augmentation methods relied on the same forward process, and a self-collected dataset would address this limitation as well. Lastly, to enhance the practicality and applicability of the NeRP method, we should move on to replicate the reconstruction in 3D space, which is more aligned with real-world clinical use cases.

Societal Impact

Our findings demonstrate that NeRP is robust enough to perform well with certain types of lower-quality priors. This has significant implications for real clinical applications, particularly in resource-constrained environments where obtaining high-quality CT scans is challenging. Firstly, available low-quality CT scans can be utilized to reconstruct high-quality images, minimizing the re-scanning effort and time for better patient outcomes. Additionally, this reconstruction capability reduces the need for extensive CT scabs, minimizing patient exposure to radiation. This reduction is particularly crucial for vulnerable populations like pediatric patients who need frequent scans and are sensitive to the cumulative effects of radiation exposure. Our findings also reveal that spatial misalignment and external factors like device bed inconsistencies pose significant challenges. These insights provide valuable considerations for deploying NeRP in real-world clinical settings and open avenues for further research to enhance its robustness.

References

An, P.; Xu, S.; Harmon, S. A.; Turkbey, E. B.; Sanford, T. H.; Amalou, A.; Kassin, M.; Varble, N.; Blain, M.; Anderson, V.; Patella, F.; Carrafiello, G.; Turkbey, B. T.; and Wood, B. J. 2020. CT Images in COVID-19 [Data set].

Antun, V.; Renna, F.; Poon, C.; Adcock, B.; and Hansen, A. C. 2020. On instabilities of deep learning in image reconstruction and the potential costs of AI. *Proceedings of the National Academy of Sciences*, 117(48): 30088–30095.

Cafaro, A.; Spinat, Q.; Leroy, A.; Maury, P.; Munoz, A.; Beldjoudi, G.; Robert, C.; Deutsch, E.; Grégoire, V.; Lepetit, V.; and Paragios, N. 2023. X2Vision: 3D CT Reconstruction from Biplanar X-Rays with Deep Structure Prior. In Greenspan, H.; Madabhushi, A.; Mousavi, P.; Salcudean, S.; Duncan, J.; Syeda-Mahmood, T.; and Taylor, R., eds., *Medical Image Computing and Computer Assisted Intervention – MICCAI 2023*, 699–709. ISBN 978-3-031-43999-5.

Gong, K.; Catana, C.; Qi, J.; and Li, Q. 2019. PET Image Reconstruction Using Deep Image Prior. *IEEE Trans Med Imagin*, 1655–1665.

Shen, L.; Pauly, J.; and Xing, L. 2022. NeRP: Implicit Neural Representation Learning With Prior Embedding for Sparsely Sampled Image Reconstruction. *IEEE Transactions on Neural Networks and Learning Systems*, 770–782.

Tancik, M.; Srinivasan, P. P.; Mildenhall, B.; Fridovich-Keil, S.; Raghavan, N.; Singhal, U.; Ramamoorthi, R.; Barron, J. T.; and Ng, R. 2020. Fourier Features Let Networks Learn High Frequency Functions in Low Dimensional Domains. In *Advances in Neural Information Processing Systems (NeurIPS)*. Curran Associates, Inc.

Zhang, H.; Capaldi, D.; Zeng, D.; Ma, J.; and Xing, L. 2022. Prior-image-based CT reconstruction using attenuation mismatched prior. *Phys Med Biol*.

Zhu, B.; Liu, J. Z.; Cauley, S. F.; Rosen, B. R.; and Rosen, M. S. 2018. Image reconstruction by domain-transform manifold learning. *Nat.*, 555(7697): 487–492.

Individual Contributions

In this section, the individual contributions and the preassigned role of each team member are outlined briefly.

- **Project Manager**: Meha Goyal

  - Tracked overall to-dos and noted any timeline issues; ran experiments for the replication method with a perfect prior and recorded results; drafted the related works section of the paper and the technical details/summary section of the slides.

- **Scribe**: Kriti Gupta

  - Kept track of meetings notes and wrote down points of discussion for later reference; implemented method for augmenting image to add Gaussian noise; ran experiments for testing priors with Gaussian noise added to the image domain; drafted extensions section including analysis of experimental results; made figure to represent how our extension fit into the NeRP pipeline.

- **Quality Control**: Sonika Potnis

  - Selected patients from publicly available dataset; aligned patient data to account for any spatial discrepancies between the prior and train images; ran experiments for NeRP method without any prior; drafted introduction of paper to effectively establish a basic understanding of our experiment's complicated concepts.

- **Assignment Manager**: Jenny Xu

  - Tracked assignment deadlines and ensured that specifications were met; implemented and ran the sparse sampling experiments; researched background and related work; organized and edited written reports to focus on key points and ensure flow, clarity, and correctness.

- **Meeting Manager**: Danny Jiang

  - Scheduled and facilitated team meetings, ensuring productive discussions and effective collaboration; set up the team's meeting minutes to prepare and organize meeting content beforehand; implemented the shifting augmentations and conducted related experiments; drafted the background section and the shifting results and analysis section of the paper, clearly communicating the project's context and findings.

- **Strategy Analyst**: Elaine Liu

  - Guided the overall project development by determining its direction and outlining the paths to achieve the objectives; proposed the timeline; closely monitored deadlines and ensured that tasks were planned and executed; coded the primary augmentation functions and demonstrated their usage to team members, fostering collaboration and understanding; discovered the device bed's being a possible noise source during experiments; drafted the methodology section of the paper; led the result analysis process for both replication & extension, effectively communicating the technical aspects of the project.

Appendix

Some additional experiment results are presented in this section for additional reference.

	Patient 1	Patient 2	Patient 3
With Prior (PSNR/SSIM)			
W/ Bed	30.01/0.795	25.25/0.490	28.57/0.649
W/O Bed	30.89/0.821	29.86/0.715	30.50/0.666
Without Prior (PSNR/SSIM)			
W/ Bed	24.39/0.537	25.59/0.550	28.42/0.672
W/O Bed	27.66/0.613	28.25/0.633	29.92/0.625

Table 5: Separate replication results of different patients; Evaluation metrics reported include PSNR in dB and SSIM values.

Augmented Prior PSNR	**Patient 1**	**Patient 2**	**Patient 3**
GausIm (PSNR/SSIM)			
41.9	25.9/0.54	21.5/0.50	21.1/0.22
45.0	25.6/0.53	20.8/0.24	25.5/0.40
49.9	25.3/0.50	19.5/0.19	21.80.22
GausSig (PSNR/SSIM)			
33.2	30.0/0.78	24.5/0.46	28.0/0.66
38.7	30.6/0.83	24.3/0.46	27.9/0.65
38.8	30.8/0.83	24.3/0.45	28.2/0.68
Sparse (PSNR/SSIM)			
38.3	30.3/0.81	25.5/0.53	26.7/0.47
40.1	29.9/0.79	24.3/0.44	28.1/0.67
40.2	30.6/0.84	25.7/0.54	28.2/0.67

Table 6: PSNR(dB) / SSIM of Reconstruction Results for 3 patients with Differing Noise Methods with the Device Bed

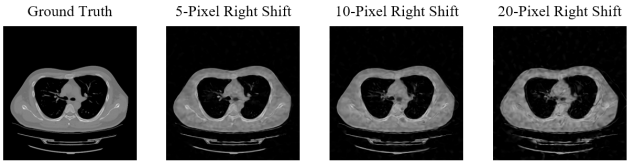

Figure 6: Reconstructed images using shifted priors compared to the ground truth